CRYSTAL GROWTH & DESIGN
2007
VOL. 7, NO. 3
580−586

Controllable Synthesis and Optical Properties of Zn-Doped CdS Nanorods from Single-Source Molecular Precursors

Yong Cai Zhang,* Wei Wei Chen, and Xiao Ya Hu

College of Chemistry and Chemical Engineering, Yangzhou University, Yangzhou City 225002, China

Received September 11, 2006; Revised Manuscript Received November 28, 2006

ABSTRACT: The controllable synthesis of hexagonal Zn-doped CdS ($Cd_{1-x}Zn_xS$, $x = 0-0.3$) nanorods from a class of solid air-stable single-source molecular precursors (cadmium zinc bis(*N*,*N*-diethyldithiocarbamate), $Cd_{1-x}Zn_x$-$(DDTC)_2$) has been achieved by two facile steps: first, $Cd_{1-x}Zn_x$-$(DDTC)_2$ ($x = 0-0.3$) was prepared directly through precipitation reactions of stoichiometric cadmium sulfate, zinc acetate, and sodium diethyldithiocarbamate in distilled water under ambient condition; second, pure hexagonal phase $Cd_{1-x}Zn_xS$ ($x = 0-0.3$) nanorods with different aspect ratios were produced via solvothermal treatment of the precursor compounds in ethylenediamine or 50 vol % ethylenediamine aqueous solution at 180 °C for 12 h. The products were characterized by powder X-ray diffraction, Raman spectroscopy, transmission electron microscopy, Fourier transform infrared spectroscopy, UV−vis absorption, and photoluminescence spectroscopy. It was observed that the optical band gap energies and photoluminescence peaks of the as-synthesized $Cd_{1-x}Zn_xS$ ($x = 0-0.3$) nanorods shift systematically toward shorter wavelengths with an increase of the Zn content; they are promising materials for photocatalysts and optoelectronic devices.

Introduction

Because of their luminescence and nonlinear optical properties, quantum size effect, and other excellent physical and chemical properties, nanocrystalline semiconductors of groups II−VI have potential applications in many technical fields, including photocatalysts, gas sensors, biological detection and imaging, solar cells, photodetectors and UV sensors, nonlinear optical materials, short-wavelength laser diodes, various luminescence devices, etc.[1−52] In solar cell systems, where CdS films have been demonstrated to be effective, the replacement of CdS with the higher band gap $Cd_{1-x}Zn_xS$ alloys has led to a decrease in window absorption losses and an increase in the short circuit current.[2,3] The ternary $Cd_{1-x}Zn_xS$ compound is also useful as a window material for the fabrication of p−n junctions without lattice mismatch in devices based on quaternary materials such as $CuIn_xGa_{1-x}Se_2$ or $CuIn(S_zSe_{1-z})$[3] and has a higher efficiency than those of pure CdS and ZnS as photocatalysts in hydrogen production.[6] $Cd_{1-x}Zn_xS$ in bulk form has a band gap which is tunable from 2.4 to 3.7 eV and, hence, can emit at different wavelengths (different band-to-band transitions) by varying the *x* values from 0 to 1. This tunability of the optical properties of ternary compound semiconductors by changing their constituent stoichiometries is superior to that by changing the particle sizes, which may cause problems in practical applications, in particular, if unstable ultrafine particles (less than ∼2 nm) are used.[20,21] Moreover, the optical properties of $Cd_{1-x}Zn_xS$ can likewise be effectively tuned through control of its phase, morphology, and size; for example, more efficient luminescence has already been achieved in ternary $Cd_{1-x}Zn_xS$, as well as in binary ZnS and CdS nanoparticles, in comparison with their bulk counterparts.[5,6,19−22] The tunability of the optical properties of $Cd_{1-x}Zn_xS$ relative to its composition, in addition to its phase, morphology, and size, should make it a more interesting material to study, considering the excitement of understanding new science and the potential hope for novel applications and even economic impacts. Unfortunately, to our knowledge, the literature reporting the synthesis and characterization of $Cd_{1-x}Zn_xS$ ($0 < x < 1$) nanostructures is limited so far.[5−12,16−21]

The conventional technique for synthesizing hexagonal phase $Cd_{1-x}Zn_xS$ powders was based on the high-temperature reactions of compositional elements or binary metal sulfides under the protection of inert gas or in vacuum, which usually yielded coarse and aggregated particles with some unwanted characteristics, such as irregular particle shape, large particle size with broad size distribution, and even inhomogeneous compositions and high impurity content. In addition, it is well-known that group II−VI materials form defects and interdiffuse at temperatures above 500 °C.[10] Therefore, the low-temperature growth of group II−VI semiconductors has gained wide acceptance.[9−11,16−22] Recently, the single-source molecular precursor (i.e., a precursor compound which contains all elements of the final material within a single-molecule)[23−25] route has opened a facile and fruitful method for the controllable synthesis of metal chalcogenide materials.[20,23−52] First of all, the single-source molecular precursor route offers the distinct advantages of mildness, safety, and simplified fabrication procedure and equipment, when compared with the use of multiple sources requiring exact control over stoichiometry, and it is especially compatible with metallorganic chemical vapor deposition (MOCVD).[23−35] Another important motivation for the use of single-source molecular precursors may be found in the observation of unusual crystal growth selectivity or metastable phase formation of the resultant products, which are sometimes unattainable via the conventional synthesis techniques.[20,36−52] To date, several single-source molecular precursors have been successfully synthesized and subsequently employed in the preparation of $Cd_{1-x}Zn_xS$ ($x = 0-1$) thin films or fine powders by means of pyrolysis in MOCVD,[23−35] in hot organic solvents,[20,36−44] in vacuum, or under the protection of inert gas.[20,44−50] But as far as we know, the large-scale production of $Cd_{1-x}Zn_xS$ ($x = 0-1$) nanorods via high-pressure solvothermal decomposition of these single-source molecular precursors has been seldom investigated.[52]

In a continuing effort, we report here the controllable synthesis of pure hexagonal phase $Cd_{1-x}Zn_xS$ ($x = 0-0.3$) nanorods from a class of easily obtained, air-stable single-source molecular precursors ($Cd_{1-x}Zn_x$-$(DDTC)_2$, $x = 0-0.3$) via subsequent solvothermal decomposition in ethylenediamine (en) or a 50 vol % en aqueous solution at a relatively low temperature

* To whom correspondence should be addressed. Phone: +86-514-7962581. Fax: +86-514-7975244. E-mail: zhangyc@yzu.edu.cn.

10.1021/cg060597f CCC: $37.00
Published on Web 02/01/2007

(180 °C). The as-synthesized products were characterized by means of powder X-ray diffraction (XRD), Raman spectroscopy, transmission electron microscopy (TEM), Fourier transform infrared spectroscopy (FT-IR), UV−vis absorption, and photoluminescence (PL) spectroscopy. In addition, the variation of product characteristics such as phase and morphology with the solvent components during solvothermal processing was investigated, and possible reasons were tentatively proposed to explain such phenomena.

Experimental Section

All the chemical reagents used in our experiments were of analytical grade and were used without further purification. The single-source molecular precursors with yields of above 85% were prepared as follows. Appropriate molar ratios of $3CdSO_4 \cdot 8H_2O$ and $Zn(CH_3COO)_2 \cdot 2H_2O$ with the sum of Cd^{2+} and Zn^{2+} mole number being 0.01 and 0.02 mol of $(C_2H_5)_2NCS_2Na \cdot 3H_2O$ were first dissolved in 100 mL of distilled water, respectively. Then, the two solutions were mixed with stirring in a 500 mL beaker. After it was stirred constantly for 5 h, the reaction solution was kept stationary at room temperature and under atmospheric pressure for 12 h. The resulting white precipitates were filtered, washed with distilled water, and dried in air at 60 °C.

In a typical procedure for the solvothermal synthesis of $Cd_{1-x}Zn_xS$, 1.000 g of the self-prepared precursor compound was put into a Teflon-lined stainless steel autoclave (50 mL capacity) to which 40 mL of en or 50 vol % en aqueous solution or distilled water was added. The autoclave was sealed and maintained at 180 °C for 12 h in an electric oven; then it was allowed to cool to room temperature naturally. The as-formed orange-yellow precipitates were filtered, washed with ethanol and distilled water several times, and dried in air at 50 °C.

Powder XRD patterns of the products were measured at a scanning speed of 0.02° s^{-1} on a German Bruker AXS D8 ADVANCE X-ray diffractometer with Cu Kα_1 radiation, in the presence of copper powders as the internal standard. Raman spectra were obtained on a Britain Renishaw Invia Raman spectrometer with a solid-state laser (excitation at 532 nm, 1 mW output power) at room temperature in the range of 200−900 cm^{-1}. The Raman spectrometer was equipped with an optical microscope and a CCD camera that can provide a good laser beam. Energy dispersive X-ray spectroscopy (EDX) analysis was performed on a Philips XL-30ESEM equipped with an EDX attachment. TEM images were taken on a Philips Tecnai-12 microscope operated at an accelerating voltage of 120 kV. FT-IR spectra were recorded on a Bruker Tensor-27 FT-IR spectrometer at room temperature with samples in a KBr wafer. UV−vis absorption spectra were obtained on a Shimadzu UV-2550 spectrophotometer with a 1 cm quartz cell. PL studies were carried out using a Japan Hitachi F-4500 fluorescence spectrophotometer at room temperature with a Xe lamp as the excitation light source. The excitation wavelength was 300 nm. The samples were ultrasonically dispersed in distilled water for both the UV−vis absorption and PL measurements.

Results and Discussion

Figure 1 shows the XRD patterns of our self-prepared precursor compounds. All of their diffraction peaks can be indexed to monoclinic structure (space group $P21/n$ [14]) of $Cd_{1-x}Zn_x$-$(DDTC)_2$ ($x = 0-0.3$), according to the JCPDS card no. 43-1978. EDX analysis results (not shown here) further revealed that these single-source molecular precursors had compositions close to the stoichiometries of the reactants used to prepare them.

Figure 2a and b shows the XRD patterns of the products derived from solvothermal treatment of the $Cd_{1-x}Zn_x$-$(DDTC)_2$ in en and 50 vol % en aqueous solution at 180 °C for 12 h, respectively. As can be seen from Figure 2a, except for the $x = 0.3$ product which contains a minor amount of CdS impurity, all the ones obtained in en displayed characteristic diffraction peaks corresponding to a hexagonal wurtzite structure (space group $P63mc$ [186]) of $Cd_{1-x}Zn_xS$ ($x = 0-0.2$) with (100), (002), (101) (102), (110), (103), (200), (112), (201), (004), and

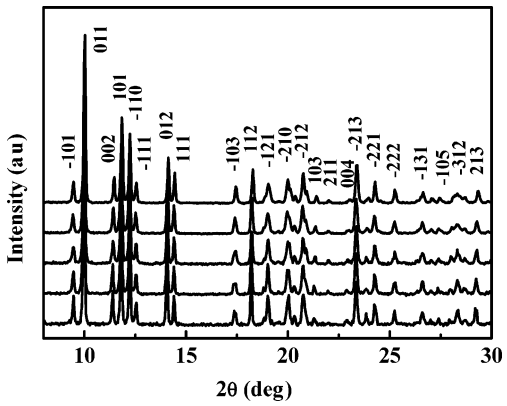

Figure 1. XRD patterns of the self-prepared single-source molecular precursors, $Cd_{1-x}Zn_x$-$(DDTC)_2$, $x = 0$, 0.05, 0.1, 0.2, and 0.3 from the bottom up.

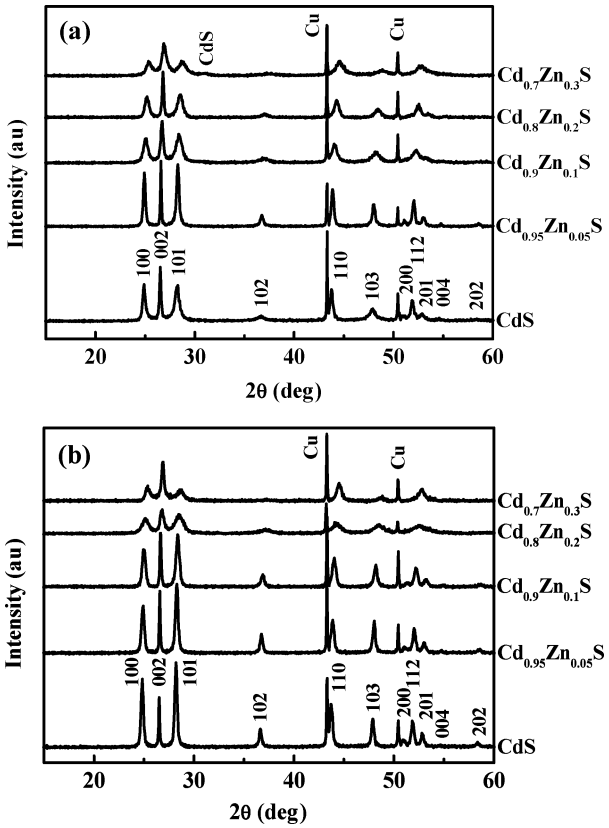

Figure 2. XRD patterns of the products derived from solvothermal treatment of the $Cd_{1-x}Zn_x$-$(DDTC)_2$ ($x = 0-0.3$) in (a) en and (b) 50 vol % en aqueous solution at 180 °C for 12 h.

(202) crystal planes. By contrast, all of the products obtained in the 50 vol % en aqueous solution were single hexagonal phase $Cd_{1-x}Zn_xS$ ($x = 0-0.3$) solid solutions, as indicated by their XRD patterns in Figure 2b. The calculated lattice parameters of the obtained hexagonal $Cd_{1-x}Zn_xS$ alloys in both solvents agreed with the corresponding literature data, as shown in Table 1. Meanwhile, the XRD peaks of the hexagonal $Cd_{1-x}Zn_xS$ synthesized in both solvents shifted gradually to larger diffraction angles as the Zn content increased, which may also rule out phase separation or separated nucleation of CdS and ZnS nanocrystals.[10,20,21] The difference in the $x = 0.3$ products obtained in the two solvents is likely caused by the greater solubility of ZnS than that of CdS in pure en, which has a stronger complexation with Zn^{2+} ions and a larger affinity with

Table 1. Comparison of the Lattice Parameters of the Hexagonal $Cd_{1-x}Zn_xS$ As Synthesized in en (denoted by superscript A) and 50 vol % en Aqueous Solution (denoted by superscript B) with the Corresponding Literature Values[a]

products	calcd params (Å)	ref params (Å)	JCPDS card no.
CdS	$a = 4.1317^A, 4.1345^B$	$a = 4.1360$	77-2306
	$c = 6.7015^A, 6.7116^B$	$c = 6.7130$	
$Cd_{0.95}Zn_{0.05}S$	$a = 4.1228^A, 4.1151^B$	$a = 4.1120$	40-0834
	$c = 6.6848^A, 6.6870^B$	$c = 6.6860$	
$Cd_{0.9}Zn_{0.1}S$	$a = 4.1096^A, 4.1072^B$	$a = 4.1044$	
	$c = 6.6763^A, 6.6695^B$	$c = 6.6674$	
$Cd_{0.8}Zn_{0.2}S$	$a = 4.0674^A, 4.0689^B$	$a = 4.0690$	40-0835
	$c = 6.6263^A, 6.6217^B$	$c = 6.6210$	
$Cd_{0.7}Zn_{0.3}S$	$a = 4.0415^B$	$a = 4.0420$	40-0836
	$c = 6.5907^B$	$c = 6.5880$	

[a] The reference lattice parameters of $Cd_{0.9}Zn_{0.1}S$ were calculated from the Vegard's Law for hexagonal $Cd_{1-x}Zn_xS$.[5]

ZnS to enter the inorganic framework.[53] This assumption may be confirmed by the fact that previous synthesis of ZnS in pure en always gave rise to a $ZnS{\cdot}(en)_{0.5}$, not ZnS,[45,53−57] while CdS could be easily produced in pure en.[37,52,58,59] Furthermore, it is worth pointing out that the doping amounts of Zn in $Cd_{1-x}Zn_xS$ can also be enhanced by choosing other appropriate solvents for the solvothermal treatment: for example, when the other conditions are kept constant and hydrazine hydrate is selected as the solvent, $Cd_{1-x}Zn_xS$ ($x = 0-1$) would be obtained, but the related work is still in progress. However, when multiple-source precursors such as stoichiometric Cd-$(DDTC)_2$ and Zn-$(DDTC)_2$, or cadmium sulfate, zinc acetate, and sodium sulfide, thioacetamide, or thiourea, were employed, instead of $Cd_{0.8}$-$Zn_{0.2}$-$(DDTC)_2$, as the reactants in the synthesis of $Cd_{0.8}Zn_{0.2}S$, with the other conditions held constant ($T = 180$ °C and $t = 12$ h), the obtained products in both solvents were not single phase $Cd_{1-x}Zn_xS$ alloys, as revealed by their XRD patterns in Figure 3 (although the XRD pattern in Figure 3a seems to be a single phase, the PL spectrum of this product in Figure 4 further discloses its mixed nature). The control experiment results clearly indicated that $Cd_{1-x}Zn_x$-$(DDTC)_2$, the single-source molecular precursors with pre-established $Cd_{1-x}Zn_x$-S chemical bonds, played an important role in attaining the alloyed $Cd_{1-x}Zn_xS$ ternary compounds under the current solvothermal conditions.

Figure 5a and b shows the room-temperature Raman spectra of the $Cd_{1-x}Zn_xS$ solid solutions prepared in en and 50 vol % en aqueous solution, respectively. Each Raman spectrum had two peaks. The first peak corresponded to a 1-LO (longitudinal optical) phonon mode and the other corresponded to 2-LO. Both the 1-LO and 2-LO peak positions of our $Cd_{1-x}Zn_xS$ products shifted continuously to higher frequencies with increasing x values (Table 2). This again suggested an alloy system in contrast to a mixture of separate CdS and ZnS phases, where no peak position shifts are expected with varying stoichiometry.[60−62] The Raman spectra of our products were also consistent with previous reports that hexagonal $Cd_{1-x}Zn_xS$ solid solutions exhibited the one-mode (i.e., LO phonon mode) type behavior, and their peak frequencies changed smoothly with composition between those of the two constituent compounds, CdS and ZnS.[60−62] On the other hand, with the increase of Zn content in the as-synthesized $Cd_{1-x}Zn_xS$, the relative intensities of both 1-LO and 2-LO peaks customarily became weaker, while the peak widths became wider, which may be related to their poorer crystallinity, shape variation, and even increased compositional and structural disorders.[60−62] In addition, the energy of the excitation light (532 nm) of the Raman spectrometer was

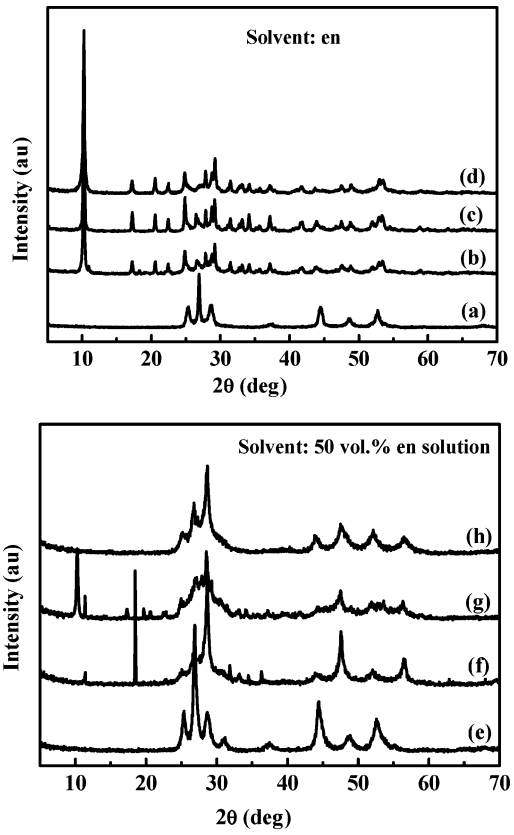

Figure 3. XRD patterns of the products derived from solvothermal reactions of stoichiometric (a) Cd-$(DDTC)_2$ and Zn-$(DDTC)_2$ or cadmium sulfate, zinc acetate, and (b) sodium sulfide, (c) thioacetamide, or (d) thiourea in en at 180 °C for 12 h, and those of the products derived from solvothermal reactions of stoichiometric (e) Cd-$(DDTC)_2$ and Zn-$(DDTC)_2$ or cadmium sulfate, zinc acetate, and (f) sodium sulfide, (g) thioacetamide, or (h) thiourea in 50 vol % en aqueous solution at 180 °C for 12 h.

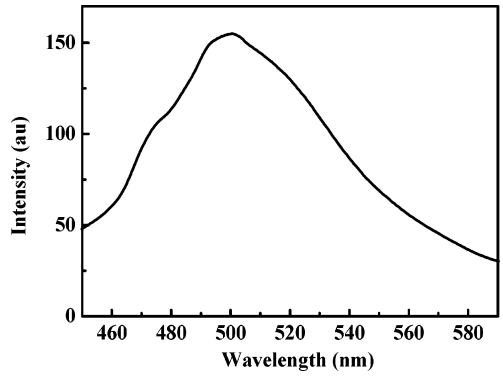

Figure 4. PL spectrum of the product in Figure 3a.

closer to the band gap of CdS, and thus the scattering intensities of $Cd_{1-x}Zn_xS$ with smaller x values were larger because of the resonance effect.

The morphology and size of the hexagonal $Cd_{1-x}Zn_xS$ alloys obtained in the two solvents were observed by TEM; the results are given in Figure 6 and Table 2. As can be seen from Figure 6a−d, the hexagonal $Cd_{1-x}Zn_xS$ ($x = 0-0.2$) products prepared in pure en consisted of almost monodisperse nanorods, which generally became slightly smaller in diameter and shorter in length with lower aspect ratios with increased x values (Table 2). On the other hand, the TEM images in Figure 6e−i indicated that the hexagonal $Cd_{1-x}Zn_xS$ ($x = 0-0.3$) products prepared

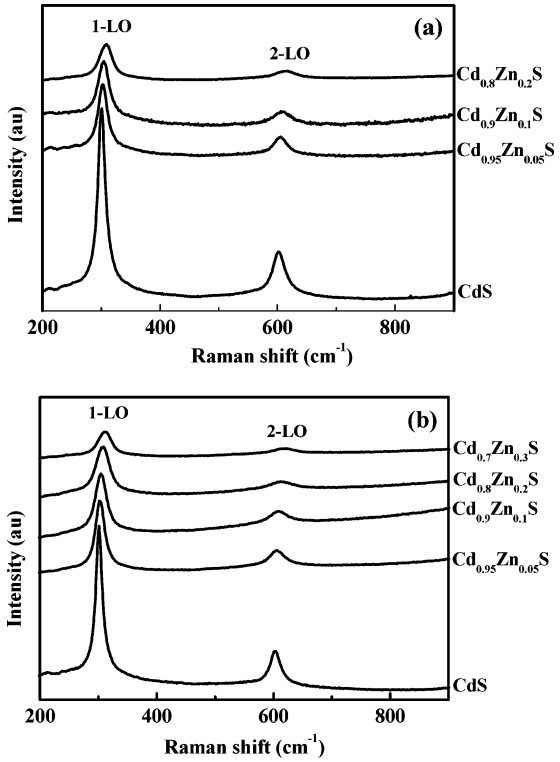

Figure 5. Raman spectra of the hexagonal $Cd_{1-x}Zn_xS$ nanorods as-prepared in (a) en and (b) 50 vol % en aqueous solution.

Table 2. Raman Peak Frequencies and Sizes (D = diameter, L = length) of the Hexagonal $Cd_{1-x}Zn_xS$ As Synthesized in en (denoted by superscript A) and 50 vol % en Aqueous Solution (denoted by superscript B)

products	1-LO peak (cm^{-1})	size observed by TEM (nm)
CdS	300.8^A, 300.9^B	$D = 20-38^A$, $18-47^B$; $L = 327-2000^A$
$Cd_{0.95}Zn_{0.05}S$	302.5^A, 302.5^B	$D = 20-34^A$, $32-55^B$; $L = 250-920^A$
$Cd_{0.9}Zn_{0.1}S$	304.6^A, 304.6^B	$D = 15-25^A$, $16-39^B$; $L = 115-360^A$
$Cd_{0.8}Zn_{0.2}S$	308.2^A, 308.0^B	$D = 11-22^A$, $15-24^B$; $L = 43-200^A$
$Cd_{0.7}Zn_{0.3}S$	311.5^B	$D = 11-22^B$

in 50 vol % en aqueous solution often comprised nanorods and nanoparticles, the diameters of which also decreased slightly with the increase of Zn content (Table 2). The slight reduction of particle diameter with increasing x values in the alloyed $Cd_{1-x}Zn_xS$ ($x = 0-0.3$) was consistent with their gradually broadening XRD patterns in Figure 2. Similar phenomena were also reported for the $Cd_{1-x}Zn_xS$ nanocrystals prepared by different methods.[6,20,21]

Although the exact mechanisms are yet undetermined, the formation of rodlike $Cd_{1-x}Zn_xS$ nanostructures in the two solvents of en and 50 vol % en aqueous solution implied that the nucleation and growth processes of $Cd_{1-x}Zn_xS$ during the solvothermal processing were well controlled. The single-source molecular precursors, $Cd_{1-x}Zn_x$-$(DDTC)_2$ ($x = 0-0.3$), can be regarded as a class of inorganic core-cluster complexes,[37,52,63,64] which would be unstable in the presence of nucleophile under suitable reaction conditions. Nucleophilic attack by the nucleophilic solvents at the thione carbon can lead to the formation of $[Cd_{1-x}Zn_xS]$ crystal nuclei.[37,52,63,64] The newly born $[Cd_{1-x}Zn_xS]$ crystal nuclei were highly active and had the tendency to combine with each other to grow into larger nanocrystals. In the course of crystal growth, these $[Cd_{1-x}Zn_xS]$ crystal nuclei may preferentially grow along a unique direction or undergo oriented aggregation and assemble into crystalline nanorods,

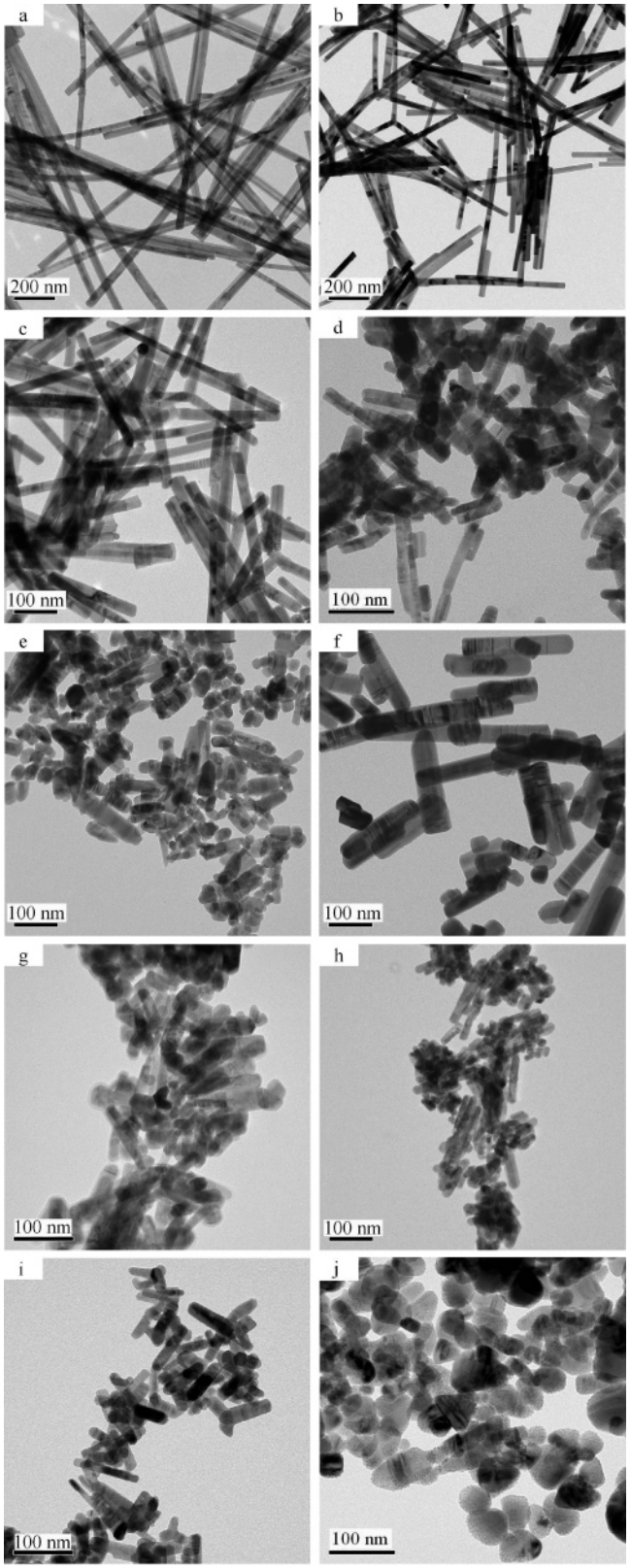

Figure 6. TEM images of the $Cd_{1-x}Zn_xS$ products with x = (a) 0, (b) 0.05, (c) 0.1, and (d) 0.2 obtained in en, those of the $Cd_{1-x}Zn_xS$ products with x = (e) 0, (f) 0.05, (g) 0.1, (h) 0.2, and (i) 0.3 obtained in 50 vol % en aqueous solution, and (j) TEM image of the CdS prepared by solvothermal treatment of the Cd-$(DDTC)_2$ in distilled water at 180 °C for 12 h.

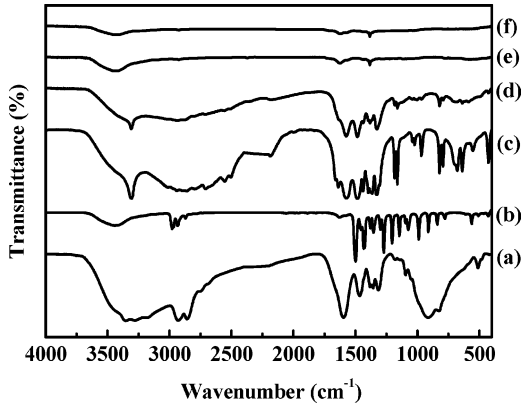

Figure 7. FTIR spectra of (a) en, (b) $Cd_{0.95}Zn_{0.05}$-$(DDTC)_2$, and the products derived from solvothermal treatment of the $Cd_{0.95}Zn_{0.05}$-$(DDTC)_2$ in en at 180 °C for (c) 0.5 and (d) 1 h without posttreatment by washing with ethanol and distilled water and FTIR spectra of the products derived from solvothermal treatment of the $Cd_{0.95}Zn_{0.05}$-$(DDTC)_2$ in en at 180 °C for (e) 0.5 and (f) 1 h after posttreatment by washing with ethanol and distilled water.

mainly under the structure-inducing effect of the bidentate solvent, as reported previously[53,58,59,65] and confirmed by our FT-IR experiments. (Figure 7 shows the typical FT-IR spectra of en, $Cd_{0.95}Zn_{0.05}$-$(DDTC)_2$, and the products obtained at different reaction times before and after posttreatment by washing with ethanol and distilled water.) As can be seen from Figure 7a−d, when the single-source molecular precursor was subjected to solvothermal treatment in en at 180 °C, its characteristic FT-IR peaks disappeared gradually with prolonging of the reaction time from 0.5 to 1 h; in contrast, the characteristic FT-IR peaks of the en molecules began to emerge in the resultant products without posttreatment by washing with ethanol and distilled water, indicating a gradual decomposition of $Cd_{0.95}Zn_{0.05}$-$(DDTC)_2$ under nucleophilic attack by en molecules. The FT-IR spectrum in Figure 7d was different from that of pure liquid en but quite similar to those of en molecules adsorbed on the sample surfaces, $CdS(en)_n$ and $ZnS(en)_n$, reported in previous literature,[53,58,59,65] implying that the en molecules had also been adsorbed onto the sample surfaces and coordinated with the surface Cd^{2+} and Zn^{2+} ions in our case. However, all the products obtained after posttreatment by washing with ethanol and distilled water did not show the presence of en, $Cd_{1-x}Zn_xS(en)_n$ and single-source molecular precursors in their FT-IR spectra (Figure 7e and f), demonstrating that our $Cd_{1-x}Zn_xS$ ($x = 0-0.3$) products were all free of organic contaminants. Because en, $Cd_{1-x}Zn_xS(en)_n$, and the single-source precursor molecules are at least soluble in distilled water or ethanol, which also agrees with the experimental results by Yang, et al.,[58] the en molecules can be adsorbed onto the surfaces of the $[Cd_{1-x}Zn_xS]$ crystal nuclei and even form the corresponding complexes with the Cd^{2+} and Zn^{2+} ions ($Cd_{1-x}Zn_xS(en)_n$, n = number). The complex ions with bidentate en ligands on the sample surfaces could be linked through hydrogen bonds in the polyamine donor solvent and self-assembled to a chain structure.[65,66] The steric hindrance, limitation of the spatial structure and the chain structure of the intermediate molecular building blocks can influence the preferential growth toward nanorods or other dendrites.[65,66] With the dilution of en via the addition of water to the 50 vol % en aqueous solution, the ability to form the chain structure intermediates via hydrogen bonds between the N of one en molecule and the H of another en molecule was greatly weakened, and hence, only shorter nanorods, as well as

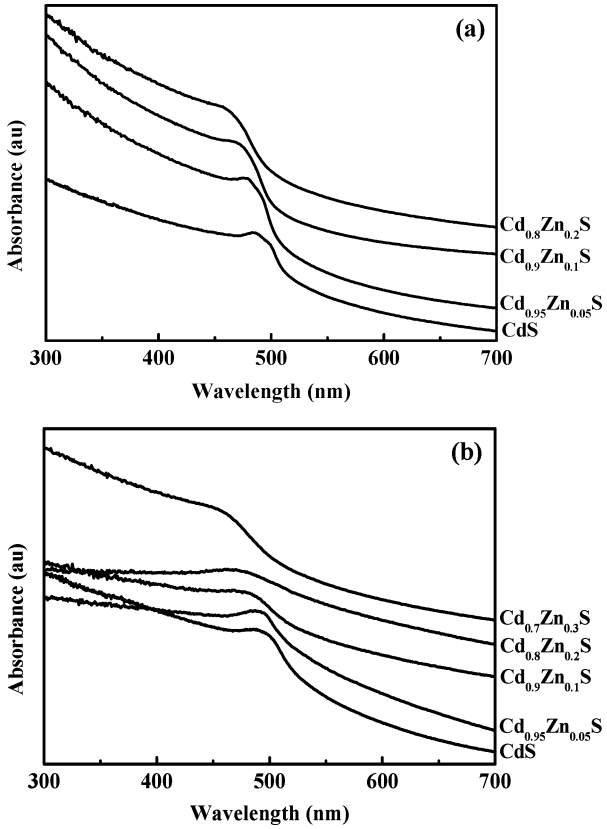

Figure 8. UV−vis absorption spectra of the hexagonal $Cd_{1-x}Zn_xS$ nanorods as prepared in (a) en and (b) 50 vol % en aqueous solution.

nanoparticles, could be formed. In case of water as the solvent, because it has no coordinating ability, only the granular nanoparticles of CdS could be formed as shown by their TEM image in Figure 6j.

Figure 8a and b shows the UV−vis absorption spectra of the hexagonal $Cd_{1-x}Zn_xS$ nanorods obtained in en and 50 vol % en aqueous solution, respectively. The optical absorption data were analyzed from the following equation to determine the band gap energies of the as-prepared ternary direct band gap semiconductors[1,6,13,14,16]

$$\alpha h\nu = B(h\nu - E_g)^{1/2}$$

where α is the absorption coefficient, $h\nu$ is the discrete photon energy, B is a constant relative to the material, and E_g is the absorption band gap. The value of the absorption coefficient can be calculated by the following equation[67]

$$\alpha = -\frac{1}{t}\ln\frac{I_t}{I_0} = \frac{1}{t}\frac{-\log\frac{I_t}{I_0}}{\log e} = \frac{1}{t}\frac{A}{\log e}$$

in which t is the thickness of the cuvette, I_t and I_0 are the intensities of transmitted light and incident light, respectively, and A is the absorbance, which can be obtained from the absorption spectra. The curves of $(\alpha h\nu)^2$ versus $h\nu$ for the as-prepared $Cd_{1-x}Zn_xS$ nanorods were plotted, and the E_g values of the products can be estimated by extrapolating the straight line portion of the plots of $(\alpha h\nu)^2$ versus $h\nu$ to $\alpha = 0$. The estimated E_g values of our products are shown in Table 3; they exhibited monotonous blue shifts with increasing Zn content but always fell within the range of the band gap energies reported for $Cd_{1-x}Zn_xS$ thin films and bulk solid solutions with

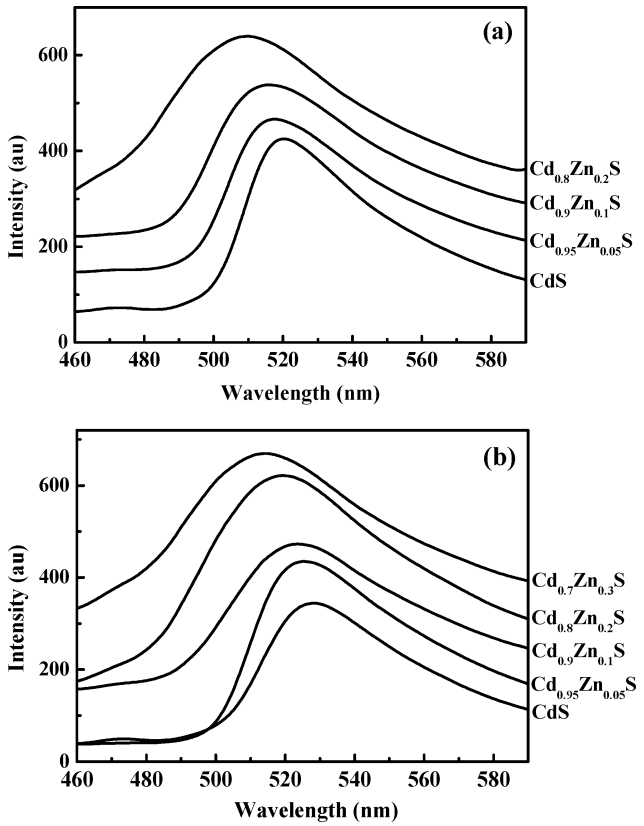

Figure 9. Room-temperature PL spectra of the hexagonal $Cd_{1-x}Zn_xS$ nanorods as prepared in (a) en and (b) 50 vol % en aqueous solution.

Table 3. Optical Properties of the Hexagonal $Cd_{1-x}Zn_xS$ As Synthesized in en (denoted by superscript A) and 50 vol % en Aqueous Solution (denoted as superscript B)

products	E_g (eV)	PL peak energy (eV)
CdS	2.42^A, 2.40^B	2.38^A, 2.35^B
$Cd_{0.95}Zn_{0.05}S$	2.47^A, 2.45^B	2.40^A, 2.36^B
$Cd_{0.9}Zn_{0.1}S$	2.51^A, 2.50^B	2.41^A, 2.37^B
$Cd_{0.8}Zn_{0.2}S$	2.60^A, 2.58^B	2.43^A, 2.39^B
$Cd_{0.7}Zn_{0.3}S$	2.69^B	2.42^B

the same compositions.[1,6,13−16,68−71] Because the particle diameters of our products were much larger than the exciton Bohr radius of $Cd_{1-x}Zn_xS$ (whose exciton Bohr radii are between those of CdS (2.2 nm) and $Cd_{0.7}Zn_{0.3}S$ (2.76 nm)),[21] no obvious quantum confinement effect took place. Therefore, the increase in E_g of the as-prepared $Cd_{1-x}Zn_xS$ nanorods with more Zn content should be attributed to the compositional modulation with negligible shape- and size-dependent effects, which is another token of the formation of the ternary $Cd_{1-x}Zn_xS$ solid solutions.[6,14,20,21]

Figure 9a and b shows the room-temperature PL spectra of the hexagonal $Cd_{1-x}Zn_xS$ nanorods obtained in en and 50 vol % en aqueous solution, respectively. It can be seen that for each sample, the PL peak energy was always lower than its corresponding band gap (Table 3). This indicated that the radiative transition occurred from the surface states rather than the excitonic transition.[5,6,7,10,18] The broad PL peaks exhibited a trend of shifting toward higher energies with increasing x values, providing additional evidence for the formation of nanocrystalline $Cd_{1-x}Zn_xS$ solid solutions.[6,7,10,18] However, the poorer crystallinity, shape variation, and even increased compositional and structural disorders of the as-prepared $Cd_{1-x}Zn_xS$ nanorods with more Zn dopants caused greater broadening and asymmetry in their PL peaks.[6]

Conclusions

Using self-prepared single-source molecular precursors $Cd_{1-x}Zn_x(DDTC)_2$ ($x = 0-0.3$), we prepared pure hexagonal phase Zn-doped CdS nanorods via subsequent solvothermal decomposition in en or 50 vol % en aqueous solution at a relatively low temperature (180 °C) and characterized them by means of XRD, Raman, TEM, FTIR, UV−vis absorption, and PL spectra. The composition-modulated optical properties of the $Cd_{1-x}Zn_xS$ nanorods may lead to the development of ideal materials for photocatalysts and optoelectronic devices. It was expected that such a simple, mild, and cheap method should be extended to prepare many other important semiconducting ternary or even quaternary metal chalcogenide nanomaterials with tunable composition, morphology, and size, only by adopting the corresponding mixed-metal diethyldithiocarbamates as their special single-source precursors.

Acknowledgment. This work is supported by the National Natural Science Foundation of China (No. 20375034), the Jiangshu Province Natural Science Foundation (No. BK2002045 and 2006072), the Yangzhou University Natural Science Foundation (No. 2006CXJ004), and the Foundation of Jiangsu Provinicial Key Program of Physical Chemistry in Yangzhou University.

References

(1) Lokhande, C. D.; Yermune, V. S.; Pawar, S. H. *Mater. Chem. Phys.* **1988**, *20*, 283−292.
(2) Morris, G. C.; Vanderveen, R. *Sol. Energy Mater. Sol. Cells* **1992**, *26*, 217−228.
(3) Gaewdang, N.; Gaewdang, T. *Mater. Lett.* **2005**, *59*, 3577−3584.
(4) Kumar, V.; Singh, V.; Sharma, S. K. *Opt. Mater.* **1998**, *11*, 29−34.
(5) Liu, Y.; Zapien, J. A.; Shan, Y. Y.; Lee, S. T. *Adv. Mater.* **2005**, *17*, 1372−1377.
(6) Bhattacharjee, B.; Mandal, S. K.; Chakrabarti, K. *J. Phys. D: Appl. Phys.* **2002**, *35*, 2636−2642.
(7) Kulkarni, S. K.; Winkler, U.; Deshmukh, N. *Appl. Surf. Sci.* **2001**, *169−170*, 438−446.
(8) Sebastian, P. J.; Ocampo, M. *Sol. Energy Mater. Sol. Cells* **1996**, *44*, 1−10.
(9) Liu, J. Z.; Yan, P. X.; Yue, G. H. *Mater. Lett.* **2006**, *60*, 3471−3476.
(10) Wang, W.; Germanenko, I.; El-Shall, M. S. *Chem. Mater.* **2002**, *14*, 3028−3033.
(11) Petrov, D. V.; Santos, B. S.; Pereira, G. A. L. *J. Phys. Chem. B* **2002**, *106*, 5325−5334.
(12) Zhai, T.; Zhang, X.; Yang, W. *Chem. Phys. Lett.* **2006**, *427*, 371−374.
(13) Innocenti, M.; Cattarin, S.; Loglio, F. *Electrochim. Acta* **2004**, *49*, 1327−1337.
(14) Padam, G. K.; Malhotra, G. L.; Rao, S. U. M. *J. Appl. Phys.* **1988**, *63*, 770−774.
(15) Salem, A. M. *Appl. Phys. A: Mater. Sci. Process.* **2002**, *74*, 205−211.
(16) Chavhan, S.; Sharma, R. P. *J. Phys. Chem. Solid* **2005**, *66*, 1721−1726.
(17) Korgel, B. A.; Monbouquette, H. G. *Langmuir* **2000**, *16*, 3588−3594.
(18) Huang, J.; Lianos, P.; Yang, Y. *Langmuir* **1998**, *14*, 4342−4344.
(19) Cizeron, J.; Pileni, M. P. *J. Phys. Chem.* **1995**, *99*, 17410−17416.
(20) Zhong, X.; Feng, Y.; Knoll, W.; M. Han. *J. Am. Chem. Soc.* **2003**, *125*, 8589−8594 and 13559−13563.
(21) Chen, D.; Gao, L. *Solid State Commun.* **2005**, *133*, 145−150.
(22) Boudjouk, P.; Jarabek, B. R.; Simonson, D. L. *Chem. Mater.* **1998**, *10*, 2358−2364.
(23) Esteves, A. C. C.; Trindade, T. *Curr. Opin. Solid State Mater. Sci.* **2002**, *6*, 347−353.
(24) Gleizes, A. N. *Chem. Vap. Deposition* **2000**, *6*, 155−173.
(25) Barreca, D.; Tondello, E.; Lydon, D. *Chem. Vap. Deposition* **2003**, *9*, 93−98.
(26) Hsu, Y.-J.; Lu, S.-Y. *Langmuir* **2004**, *20*, 194−201.
(27) Nyman, M.; Hampden-Smith M. J.; Duesler, E. N. *Chem. Vap. Deposition* **1996**, *2*, 171−174.

(28) Tran, N. H.; Lamb, R. N. *J. Phys. Chem. B* **2000**, *104*, 1150−1152.
(29) Bradley, D. C. *Chem. Rev.* **1989**, *89*, 1317−1322; *Polyhedron* **1994**, *13*, 1111−1121; *Appl. Surf. Sci.* **1990**, *46*, 1−4.
(30) Frigo, D. M.; Khan, O. F. Z.; O'Brien, P. *J. Cryst. Growth* **1989**, *96*, 989−992.
(31) Bochmann, M. *Chem. Vap. Deposition* **1996**, *2*, 85−96.
(32) O'Brien, P.; Walsh, J. R.; Watson, I. M. *J. Cryst. Growth* **1996**, *167*, 133−142.
(33) Nomura, R.; Murai, T.; Toyosaki, T. *Thin Solid Films* **1995**, *271*, 4−7.
(34) Ajayi, O. B.; Osuntola, O. K. *Thin Solid Films* **1994**, *248*, 57−62.
(35) Nyman, M.; Jenkins, K.; Hampden-Smith M. J. *Chem. Mater.* **1998**, *10*, 914−921.
(36) Malik, M. A.; O'Brien, P.; Revaprasadu, N. *Chem. Mater.* **2001**, *13*, 913−920; **2002**, *14*, 2004−2010.
(37) Yan, P.; Xie, Y.; Qian, Y. *Chem. Commun.* **1999**, 1293−1294.
(38) Jun, Y.; Cheon, J. *J. Am. Chem. Soc.* **2001**, *123*, 5150−5151; **2002**, *124*, 615−619.
(39) Tong, H.; Zhu, Y.-J. *Nanotechnology* **2006**, *17*, 845−857.
(40) Pradhan, N.; Efrima, S. *J. Am. Chem. Soc.* **2003**, *125*, 2050−2051.
(41) Nair, P. S.; Radhakrishnan T.; Revaprasadu, N.; O'Brien P. *Polyhedron* **2003**, *22*, 3129−3135; *Chem. Commun.* **2002**, 564−565; *J. Mater. Chem.* **2001**, *11*, 1555−1556.
(42) Cumberland, S. L.; Hanif, K. M.; Strouse, G. F. *Chem. Mater.* **2002**, *14*, 1576−1584.
(43) Trindade, T.; O'Brien, P.; Zhang, X. *Chem. Mater.* **1997**, *9*, 523−530.
(44) Brennan, J. G.; Siegrist, T.; Carroll, P. J. *J. Am. Chem. Soc.* **1989**, *111*, 4141−4143; *Chem. Mater.* **1990**, *2*, 403−409.
(45) Yu, S. H.; Yoshimura, M. *Adv. Mater.* **2002**, *14*, 296−300.
(46) Malandrino, G.; Finocchiaro, S. T.; Rossi, P. *Chem. Commun.* **2005**, 5681−5683.
(47) Barrelet, C. J.; Wu, Y.; Bell, D. C. *J. Am. Chem. Soc.* **2003**, *125*, 11498−11499.
(48) Zeng, D.; Hampden-Smith, M. J. *Polyhedron* **1994**, *13*, 2715−2730.
(49) Osakada, K.; Yamamoto, T. *Inorg. Chem.* **1991**, *30*, 2328−2332.
(50) Takahashi, Y.; Yuki, R.; Sugiura, M. *J. Cryst. Growth* **1980**, *50*, 491−497.
(51) Liu, W. *Mater. Lett.* **2006**, *60*, 551−554.
(52) Zhang, Y. C.; Wang, G. Y.; Hu, X. Y. *J. Cryst. Growth* **2005**, *284*, 554−560; *Mater. Res. Bull.* **2006**, *41*, 1 817−1824; *J. Alloy. Comp.* [Online early access] DOI: 10.1016/j.jallcom.2006.07.065. Published Online: Aug 21, 2006.
(53) Deng, Z. X.; Wang, C.; Li, Y. D. *Inorg. Chem.* **2002**, *41*, 869−873.
(54) Dai, J.; Jiang, Z.; Li, W. *Mater. Lett.* **2002**, *55*, 383−387.
(55) Li, C.; Yang, X.; Yang, B. *J. Cryst. Growth* **2006**, *291*, 45−51.
(56) Chen, X.; Xu, Y.; Xu, N. *Inorg. Chem.* **2003**, *42*, 3100−3106.
(57) Yu, S. H.; Yang, J.; Qian, Y. T. *Chem. Phys. Lett.* **2002**, *361*, 362−366.
(58) Yang, J.; Yu, S. H.; Qian, Y. T. *Chem. Mater.* **2000**, *12*, 3259−3263.
(59) Ma, X.; Xu, F.; Zhang, Z. *Mater. Res. Bull.* **2005**, *40*, 2180−2188.
(60) Ichimura, M.; Furukawa, T.; Shirai, K. *Mater. Lett.* **1997**, *33*, 51−55.
(61) Ichimura, M.; Usami, A.; Wada, T. *Phys. Rev. B* **1992**, *46*, 4273−4276.
(62) Shamir, J.; Larach, S. *Spectrochim. Acta, Part A* **1971**, *27*, 2105−2108.
(63) Domenicano, A.; Torelli, L.; Vaciago, A. *J. Chem. Soc. A* **1968**, 1351−1352.
(64) Ramadas, K.; Janarthanan, N. *J. Chem. Res., Synop.* **1998**, 228−229.
(65) Gorai, S.; Ganguli, D.; Chaudhuri, S. *Mater. Sci. Eng. B* **2005**, *116*, 221−225; *Cryst. Growth Des.* **2005**, *5*, 875−877.
(66) Li, B.; Xie, Y.; Huang, J. *Nanostruct. Mater.* **1999**, *11*,1067−1071.
(67) Khiew, P. S.; Radiman, S.; Huang, N. M. *J. Cryst. Growth* **2003**, *254*, 235−243.
(68) Kwok, H. L. *J. Phys. D: Appl. Phys.* **1983**, *16*, 2367−2377.
(69) Gunasekaran, M.; Ramasamy, P.; Ichimura, M. *J. Electrochem. Soc.* **2006**, *153*, G664−668.
(70) Kuhaimi, S. A. A.; Tulbah, Z. *J. Electrochem. Soc.* **2000**, *147*, 214−218.
(71) Ballentyne, D. W. G.; Ray, B. *Physica* **1961**, *27*, 337−341.

CG060597F